# Local Crack Branching as a Mechanism for Instability in Dynamic Fracture

Eran Sharon,[1] Steven P. Gross,[2] and Jay Fineberg[1]

[1]*The Racah Institute of Physics, The Hebrew University of Jerusalem, Givat Ram, Jerusalem, Israel*

[2]*The Center for Nonlinear Dynamics, The University of Texas, Austin, Texas 78712*

(Received 7 February 1995)

The motion of a crack in dynamic fracture has been shown to be governed by a dynamical instability causing oscillations in its velocity and structure on the fracture surface. We present experimental evidence indicating that the mechanism for instability is attempted local crack branching. At the instability onset, a crack will locally change its topology and sprout small, microscopic side branches. The trajectories of these local branches are independent of the crack velocity and exhibit scaling behavior. A connection between microscopic and macroscopic crack branching is established.

PACS numbers: 68.35.Gy, 62.20.Mk, 83.50.Tq

The dynamic behavior of cracks propagating through brittle, amorphous material has been the object of much recent interest. In the study of crack propagation, we drive a system having many degrees of freedom far from its equilibrium configuration. We then ask the very basic question of how the system chooses to dispose of this externally imposed energy. In the presence of a crack, an elastic solid will collectively focus energy stored in its elastic deformation field creating a (nearly) singular stress field at the crack's tip. At a critical value of applied stress, the crack will start to propagate, both relieving the stress built up in the surrounding material and converting the energy flowing into its tip to the new surface. We will demonstrate that at a critical velocity, $v_c$, this system chooses to develop a new mode of dissipation. It diverts this energy to not a single crack, but to the formation of additional branches. Branching is a general phenomenon, occurring in other systems (e.g., dielectric breakdown or electrodeposition), described by a moving interface driven by a singular field. Thus, our results may be relevant to this general class of nonlinear systems.

Recent experimental work [1] has shown that a dynamic instability controls a crack's advance when its velocity exceeds a critical velocity, $v_c$, of $0.36V_R$, where $V_R$ is the Rayleigh wave speed in the material. Beyond $v_c$ the crack dynamics change dramatically. At that point, the mean acceleration of the crack drops, the crack velocity starts to oscillate, and a pattern correlated with the velocity oscillations is created on the fracture surface. Whereas the initial experiments were performed on PMMA (a brittle polymer), additional experiments monitoring the acoustic emissions in both PMMA and soda-lime glass [2] demonstrated the general nature of the observed instability.

Much recent theoretical work has been devoted to understanding the origin of the instability. Phenomenological model equations [3] yields, in 1D, oscillations of the crack tip velocity above a critical crack speed [4]. Recent work in a 2D isotropic elastic medium [5] using a viscous dissipation term defined on the fracture surface [6] indicates that the principle stress normal to the direction of propagation surpasses the parallel stress component beyond a dissipation-dependent critical velocity. Thus, above this velocity the straight-line path of a crack is unstable. Similar behavior at a single critical velocity of $0.6V_R$ was first observed by Yoffe [7], using 2D linear elastic theory with no dissipation.

A different approach to the problem was taken by Marder and Liu [8] by modeling the elastic medium as a 2D lattice of coupled springs. Brittle behavior is modeled by allowing a spring to be elastic until a critical displacement at which time they snap. To simulate dissipation, a small viscous term is introduced. The model reproduces the Yoffe instability; solutions propagating in a straight line are unstable above a velocity of about $0.6V_R$. Moreover, numerical solutions of the model for $v > 0.6V_R$ exhibit the periodic occurrence of local branching events where the main crack sprouts side branches that propagate for a short distance and die. The spacing between these "frustrated" branches is a function of the amount of dissipation. Attempted crack branching has also been observed in recent simulations of crack motion using molecular dynamics [9].

In this paper we find experimentally that the crack indeed bifurcates (branches) beyond the critical velocity for the onset of the velocity oscillations. The crack velocity then becomes a well-defined function of the local branch length. We then consider the character of the local branches as they develop. We find that, surprisingly, the functional form of a given branch is independent of the mean crack velocity and can be described by a power law function of its projection in the propagation direction of the main crack. Thus, the "branching angle" of a given branch is not well defined, but rather a function of the scale at which the angle is measured.

The experimental apparatus is similar to that described in [1]. Our experiments were conducted in thin, quasi-2D sheets of brittle, cast PMMA [10] having a thickness of either 0.8 or 3 mm with vertical (parallel to the direction of applied stress or "$Y$" direction) and horizontal (parallel to the propagation or "$X$" direction) dimensions

 0031-9007/95/74(25)/5096(4)$06.00 © 1995 The American Physical Society

between 50–200 and 200–400 mm, respectively. Stress was applied to all samples via uniform displacement of the vertical boundaries with the fracture initiated at constant displacement. Applied stresses in the experiment were varied between 10 and 18 MPa. Upon fracture initiation, the location of the crack tip was measured as in [1] at 0.1 $\mu$s intervals with a 0.1 mm spatial resolution yielding a velocity resolution of better than 25 m/s.

After fracture, the crack profile in the $X$-$Y$ plane was measured optically with a spatial resolution of 1–5 $\mu$m depending on the magnification used. The optical measurements were then correlated with the velocity measurements. Although the medium is idealized as 2D, the plates used are of finite thickness. All comparisons between local branches and the crack velocity were made using branches adjacent to the plane where the velocity measurements were performed.

Typical profiles of local crack branches observed in the $X$-$Y$ plane are presented in Fig. 1. For crack velocities less than $v_c = 330$ m/s [Fig. 1(a)], the fracture profile is featureless and the fracture surface has a smooth mirrorlike character. Beyond $v_c$ microscopic "daughter" cracks appear, as shown in Fig. 1(b). As the mean crack velocity increases still further, these daughter cracks appear in bunches [Fig. 1(c)] where the length of an individual daughter crack in a given bunch can vary considerably. The spacing between groups of daughter cracks corresponds to the spacing between the velocity fluctuations of the crack. As $v$ increases still further, the structure of the local branches becomes increasingly complicated as revealed in Fig. 1(d). The local branches observed, up to and including areas where surface patterns are visible, have a finite width and, generally, do not extend throughout the entire thickness of the plate.

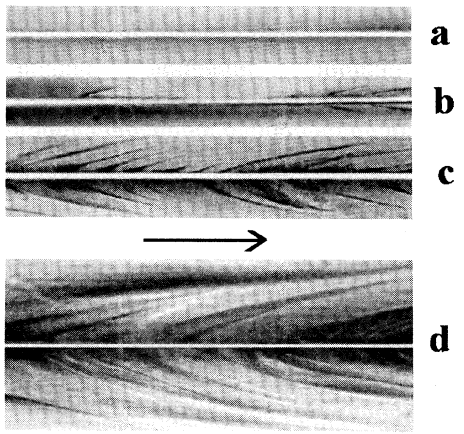


FIG. 1. Examples of local crack branching images in the $X$-$Y$ plane. The arrow, of length 0.25 mm, indicates the direction of propagation. All figures are to scale and the path of the main crack in each image is in white. (a) $v < v_c = 330$ m/s, (b) $v = 340$ m/s, (c) $v = 400$ m/s, and (d) $v = 480$ m/s.

How are the dynamics of the crack dependent on the existence of local branches? Figure 2 compares the mean crack velocity (smoothed over 5 mm to reduce the fluctuating part) with the average length of the local branches in the same interval. Prior to $v_c$ local branching is nearly nonexistent. For $v > v_c$ the dynamics of the crack are highly correlated with the length of the branches. A plot of mean local branch lengths as a function of the mean crack velocity is presented in Fig. 3 using data obtained from experiments exhibiting different acceleration rates and initial conditions. Both a sharp transition at $v_c$ together with a high degree of reproducibility are evident.

Figure 4 compares the instantaneous crack velocity with the local (averaged over a 0.1 mm interval) branch lengths. A rough correlation between the velocity fluctuations and the onset of local branches is apparent. The degree of correlation is influenced by branching events in $X$-$Y$ planes away from the sample edge and not considered here. The data in Fig. 4 were obtained for crack velocities marginally above $v_c$ when the branching patterns are relatively simple [as in Fig. 1(b) or 1(c)]. At this stage, the patterns observed on the fracture surface at higher velocities are not evident, although one still sees evidence in the figure of the periodicity in both the velocity and generation of the branches. At higher crack velocities [Fig. 1(c)], due to the complicated branched structures that are formed, the periodicity of the branching pattern is not directly evident and can only be seen by looking at the branch density.

The above results suggest an explanation for the velocity fluctuations of the crack. As the crack accelerates, the energy released from the potential energy stored in the plate is channeled into creating new surfaces (the two crack faces). When the crack velocity reaches $v_c$, the critical velocity for the onset of branching, the energy flowing

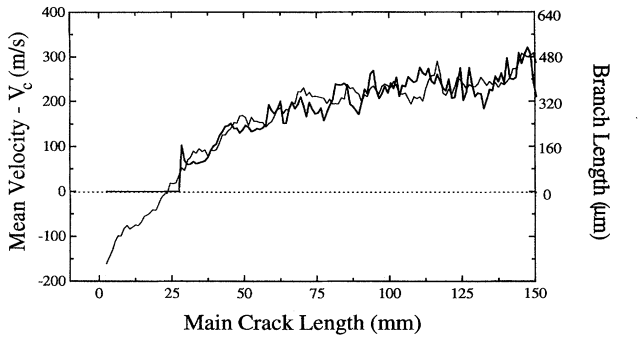


FIG. 2. A comparison of the branch length with the mean crack velocity. The velocity measurements (thin line) were smoothed by performing a running average over a distance of 5 mm. The mean branch length (bold line) was obtained by averaging local measurements over the same interval. To facilitate comparison, the critical velocity, $v_c$, for the onset of the instability was subtracted from the mean velocity measurements.

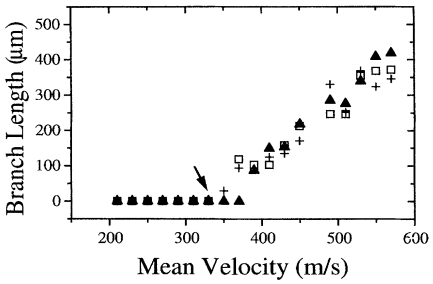


FIG. 3. The mean branch length as a function of the mean crack velocity (both smoothed as in Fig. 2) for three experimental runs where fracture occurred at different external stresses. Note the sharp transition at $v_c$ (arrow).

into the tip of the crack is now divided between the main crack and the daughter cracks. Thus, less energy is directed into the main crack and its velocity decreases. The daughter cracks, who compete with the main crack, have a finite lifetime, presumably because the main crack can "outrun" them and screen the daughter cracks from the surrounding stress field. The daughter cracks then die and the energy that had been diverted from the main crack returns, causing it to accelerate until, once again, the scenario repeats itself. Both the mean crack velocity and mean crack length are determined by the amount of energy flowing into the crack tip; more energy results in a higher mean crack velocity and longer branch length, as can be seen in Fig. 3.

As shown in Fig. 1, the local branches, in general, do not appear as a single side branch but in bunches that become progressively more complex as the mean crack velocity increases. At a given mean crack velocity the lengths of individual branches can vary by over an order of magnitude. The variation of lengths may be due to an initial distribution of defects of microcracks who feel the singular stress field ahead of the main crack. Since the activation energy for crack initiation depends on the initial size of the crack, we might expect a distribution

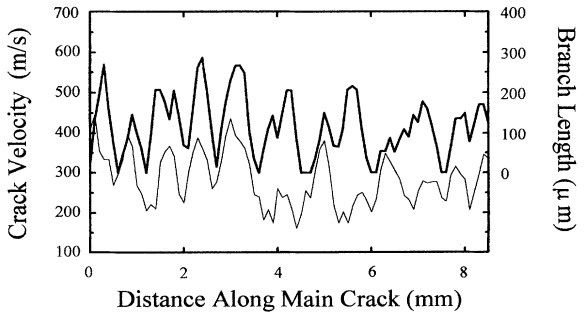


FIG. 4. A comparison of local velocity (bold line) and branch length (thin line) measurements. The data are roughly correlated and oscillate over the same (~1 mm) scale.

in both the number and lengths of the daughter cracks to emerge.

We now turn to the functional form of these branches. Figure 5(a) demonstrates that an ensemble of branches, occurring at the same mean crack velocity when superimposed, trace out a well-defined curve. For crack velocities within 10% of $v_c$, this curve exhibits remarkably little scatter. The scatter increases with increasing crack velocity reaching several times the measurement uncertainty at velocities 40% over $v_c$. [The scatter for low velocities [Fig. 5(a)] is on the order of the $\pm 3$ $\mu$m uncertainty in the starting point of a given branch.] In the inset of Fig. 5(a) we compare the mean branch profile for different mean crack velocities obtained by averaging ensembles of branches occurring within 5% of a given velocity. The profile shows little dependence on the crack velocity.

We now consider the branching angle of the crack, defined as the initial angle between a branched crack and the direction of propagation of the main crack. Past experiments have observed that the macroscopic branching angle [11] falls in the range of 10°–15°. Although often observed, a first principles understanding of crack branching, including a well-defined criterion for the appearance

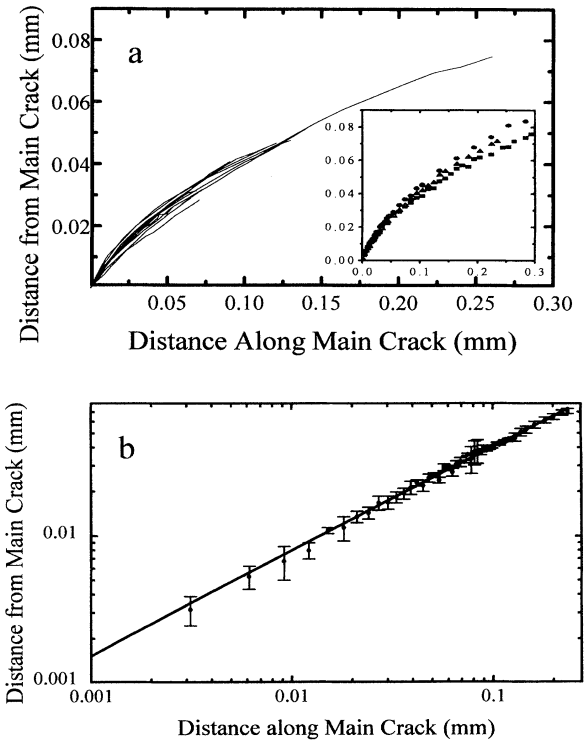


FIG. 5. (a) A superposition of 12 different local branches occurring at a mean crack velocity of 37 m/s. Inset: The mean form of local branches obtained for different propagation velocities: circles 407 m/s, triangles 374 m/s, and squares 471 m/s. (b) Comparison of the mean branch profiles (circles) at $v = 374$ m/s with power-law scaling behavior (solid line).

of crack branches together with a description of the branching angle, is lacking. There are a number of predictions for this angle in the literature. The Yoffe calculation [8] predicts an angle of 60°, branching angles of 30° were observed in molecular simulations [12], and an angle of 18° was predicted [13] using an energy criterion and considering nonsingular terms of the stress field, relevant away from the vicinity of the crack tip.

We might expect the trajectory that a branch chooses to be related to the (singular) stress field in the near vicinity of the crack tip. This could lead to singular (scale-invariant) behavior of the crack profile. Figure 5(b) presents a comparison of a mean crack profile with the scaling function obtained from the power-law fit $y = 0.20x^{0.70}$. Here $x$ is the coordinate in the propagation direction of the main crack and $y$ the normal distance from that axis. This form provides a good description of the crack profile down to the smallest scales measured [14].

We can now understand the relation between observed macroscopic crack branching and the microscopic crack branching driving instability at $v > v_c$. The functional form of the crack branch profile suggests that the observed "branching angle" is a function of the scale at which an observation is made. At scales of 0.1–0.3 mm the branching profile would indeed produce apparent branching that would fall within the range noted in the literature. The *apparent* branching angle at the smallest scale observed in our experiments (on the order of 5–10 $\mu$m) is about 30°, in agreement with molecular simulations [12], but at still smaller scales we might expect to see an even larger angle.

The power-law form of a local branch may provide an explanation for the scaling behavior of a fracture surface that has been observed in many materials [15]. The roughness of a fracture surface, $\sigma$, is defined as the rms deviation of the surface height from its mean value. A number of recent experiments have observed that $\sigma \sim L^{\zeta}$ where $L$ is the measurement scale. The measured value of 0.7 for the "roughness exponent," $\zeta$, has been conjectured to be universal in brittle two-dimensional materials [16].

Using the scaling relation $y = x^{0.7}$ for the functional form of a branch, one can derive, for scales smaller than the typical spatial extent of a local branch, a roughness exponent of 0.7 corresponding to these measurements. Our work would suggest that the region where the surface roughness is observed to exhibit scaling behavior may be limited to these scales and thus (see Fig. 3) is a function of the crack's velocity or alternatively the energy dissipated by the system.

In conclusion, our measurements suggest that the instability mechanism governing the behavior of a moving crack is that of local crack branching. At $v_c$, the critical velocity for the onset of velocity oscillations, a crack will emit microscopic, short-lived local branches. The length of these branches correlates well with the mean dynamics of the crack. We found that the power-law form of the local branches provides both a link between the dynamic instability of crack motion and the branching angles observed when branches become macroscopic in length and a possible explanation for the scaling behavior observed in fracture surface roughness. Branching also allows the crack to greatly increase its energy dissipation by creating additional fracture surface. This causes both "velocity dependence" in the energy needed to create new surface, and "low" values for the terminal crack velocity [17].

We are left with a number of questions. Theoretical models predict some of the qualitative features seen in the experiments. Quantitative agreement with theory on key points such as the value of $v_c$, the time scale for the oscillations, and the form that the branches take is still lacking. In addition, questions such as the role of dissipation, predictions for the branch lifetime, and at what stage a branch will eventually break away from the main crack remain to be addressed.

This work was supported by the United States–Israel Binational Science Fund (Grant 92-148).

[1] J. Fineberg, S. P. Gross, M. Marder, and H. L. Swinney, Phys. Rev. Lett. **67**, 457 (1992); Phys. Rev. B **45**, 5146 (1992).
[2] S. P. Gross, J. Fineberg, W. D. McCormick, M. Marder, and H. L. Swinney, Phys. Rev. Lett. **71**, 3162 (1993).
[3] J. S. Langer, Phys. Rev. A **46**, 3123 (1992).
[4] K. Runde, Phys. Rev. E **49**, 2597 (1994).
[5] E. Ching, Phys. Rev. E **49**, 3382 (1994).
[6] J. S. Langer, Phys. Rev. Lett. **70**, 3592 (1993).
[7] E. H. Yoffe, Philos. Mag. **42**, 739 (1951).
[8] M. Marder and X. Liu, Phys. Rev. Lett. **71**, 2417 (1993).
[9] F. F. Abraham, D. Brodbeck, R. A. Rafey, and W. E. Rudge, Phys. Rev. Lett. **73**, 272 (1994).
[10] The PMMA used has the following properties: Young's modulus = $3.1 \times 10^3$ MPa, Poisson ratio = 0.35, and $V_R$ = 926 m/s.
[11] For PMMA, see B. Cotterell, Appl. Mater. Res., 227 (1965). In homalite-100 and polycarbonate, see M. Ramulu and A. S. Kobayashi, Int. J. Fract. **27**, 187 (1985). In glass see J. W. Johnson and D. G. Holloway, Philos. Mag. **17**, 899 (1968).
[12] Branching at 30° was observed in [9], but this may correspond to the direction of symmetry of the hexagonal lattice used in the simulation.
[13] P. S. Theocaris and H. Georgiadis, Int. J. Fract. **29**, 181 (1985); J. G. Michopoulos and P. S. Theocaris, Int. J. Engng. Sci. **29**, 13 (1991).
[14] Measurements at smaller scales than 2–3 $\mu$m were limited by both the diffraction limit of the lenses and the diffraction patterns formed by the crack itself.
[15] See, for example, K. J. Maloy, A. Hansen, E. L. Hinrichsen, and S. Roux, Phys. Rev. Lett. **68**, 213 (1992).
[16] T. Enjoy, K. J. Maloy, A. Hansen, and S. Roux, Phys. Rev. Lett. **73**, 834 (1994); J. Kertesz, V. Horvath, and F. Weber, Fractals **1**, 67 (1993); A. Hansen, E. L. Hinrichsen, and S. Roux, Phys. Rev. Lett. **66**, 2476 (1991)
[17] E. Sharon, S. P. Gross, and J. Fineberg (to be published).

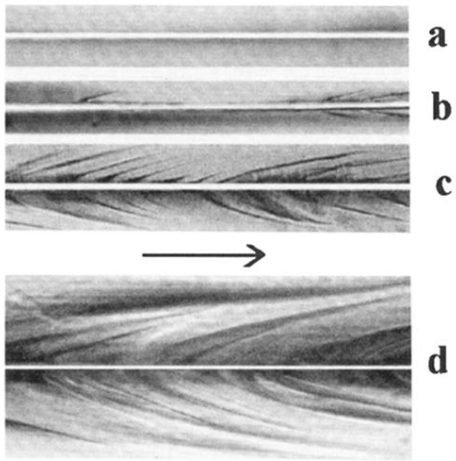


FIG. 1. Examples of local crack branching images in the $X$-$Y$ plane. The arrow, of length 0.25 mm, indicates the direction of propagation. All figures are to scale and the path of the main crack in each image is in white. (a) $v < v_c = 330$ m/s, (b) $v = 340$ m/s, (c) $v = 400$ m/s, and (d) $v = 480$ m/s.